DOI: 10.1002/ejic.200700850

Critical Effect of Phosphane Ligands on the Mechanism of Carbon–Carbon Bond Formation Involving Palladium(II) Complexes: A Theoretical Investigation of Reductive Elimination from Square-Planar and T-Shaped Species

Valentine P. Ananikov,*[a,b] Djamaladdin G. Musaev,[b] and Keiji Morokuma[b]

Keywords: C–C coupling / Palladium / Catalysis / Steric effect / Electronic effect / Phosphane ligands

A theoretical ONIOM study has been carried out to understand the influence of phosphane ligands on the structure of Pd complexes and their reactivity in C–C bond formation. The calculations were performed for Me–Me reductive elimination with the ligands L = PPh_3, PCy_3, PMe_3, PH_3, and vinyl–vinyl, Ph–Ph, ethynyl–ethynyl, vinyl–Me, vinyl–Ph and vinyl–ethynyl couplings with L = PPh_3 for $[PdR_2L_n]$ complexes (n = 1, 2). The calculations revealed critical changes in the reactivity of palladium complexes depending on the mechanism and ligand type. In the case of the standard four-coordinate pathway (n = 2) the relative reactivity in carbon–carbon bond formation follows the order: L = PPh_3 > PH_3 > PCy_3 > PMe_3. However, for reductive elimination involving T-shaped complexes by the ligand predissociation pathway (n = 1), the relative reactivity changes in the order: L = PCy_3 > PPh_3 > PH_3 > PMe_3. The theoretical study suggested that the steric effect of phosphane ligands has the largest impact on the structure of the initial palladium complexes, while the electronic effect is most influential on the transition states of C–C coupling in these complexes.

1. Introduction

Palladium-catalyzed reactions have had a major impact on developing new synthetic methods for C–C and C–X bond formation.[1–4] On several reactions it was established that the choice of an appropriate phosphane ligand for the palladium complex plays a crucial role in creating and optimizing new catalytic methodologies.[1,2] Utilization of organic chlorides (aryl chlorides, etc.)[5] in cross-coupling reactions is an outstanding recent example of tuning catalytic activity by steric and electronic effects of ligands. The key finding was to carry out the cross-coupling reaction with very electron-rich ligands.[6,7] Undoubtedly, further development of the field strongly depends on our understanding of reaction mechanisms and rationalization of the influence of phosphane ligands, especially on the reactivity of the intermediate metal complexes involved in these catalytic transformations.[8,9]

Different approaches, including IR frequencies, NMR chemical shifts and coupling constants, electronic density distribution, etc.,[10,11] have been developed to characterize steric and electronic effects of phosphane ligands on the ground-state geometry of transition-metal complexes. An attempt has been made to correlate structural and energetic properties of Pt and Pd complexes with steric and electronic properties of phosphane ligands.[12] In contrast to ground-state properties, predicting the reactivity of transition-metal complexes is a much more challenging problem. A recent study has suggested the MESP (Molecular Electrostatic Potential) approach to characterize the electron-donating ability of phosphane ligands.[13] A later work criticized this approach and concluded that MESP is unsubstantiated for characterizing the donating ability of phosphanes.[14] However, a further analysis again provided some evidence that MESP could be a good measure of the electron-donating ability of phosphanes.[15,16] Finally, a recent review on the subject made uncertain conclusions concerning the usage of modern theoretical methods to deal with the problem.[16] This example clearly emphasizes the complexity of the question and indicates the necessity of a clarifying study in this fascinating field.

[a] N. D. Zelinsky Institute of Organic Chemistry, Russian Academy of Sciences,
Leninsky Prospect 47, Moscow 119991, Russia
Fax: +7-4951355328
E-mail: val@ioc.ac.ru
[b] Cherry L. Emerson Center for Scientific Computation and Department of Chemistry, Emory University,
Atlanta, Georgia 30322, USA
Supporting information for this article is available on the WWW under http://www.eurjic.org or from the author.

A very important question concerns the nature of transition-metal complexes involved in the reductive elimination reaction. In a number of experimental reports it has been proposed that phosphane ligand dissociation accelerates C–C and C–X bond formation on Pd and Pt complexes (via T-shaped intermediates).[17,18] A computational study performed for the C–H reductive elimination reaction from Pt complexes with model PH_3 and PMe_3 ligands has suggested, however, that direct reductive elimination without ligand dissociation is preferred for four-coordinate complexes.[19] The study raises a question concerning the relative reactivity of four-coordinate vs. three-coordinate complexes in C–C bond formation.

The above discussion reveals a rather complex picture of C–C bond formation on transition-metal complexes with strong dependence on the complex type, substituents and ligand environment, which may not find a concise explanation based on available mechanistic knowledge. So far, only simple PH_3 and PMe_3 ligands were mostly utilized in theoretical studies of C–C bond-formation reactions.[20–25] However, detailed investigation of the systems with real-size ligands is required to link available experimental data with computations.

In the present study we have evaluated the effect of phosphane ligands on C–C bond formation from Pd^{II} complexes (Scheme 1) through the reductive elimination mechanism (**1** → **2-TS** → **3**) involving four-coordinate initial complexes as well as the dissociative pathway (**4** → **5-TS** → **3**) involving three-coordinate species. We have calculated the most frequently used triphenylphosphane ligand (PPh_3) and trialkylphosphanes (PMe_3 and PCy_3) with different bulkiness of the organic groups. For comparative purpose, we have also calculated the PH_3 model ligand widely used in earlier theoretical studies.

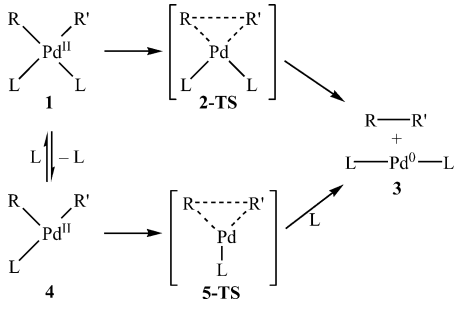

Scheme 1. Carbon–carbon coupling through four-coordinate and three-coordinate mechanisms; R, R′ = CH_3, $CH{=}CH_2$, C_6H_5, C≡CH; L = PH_3, PMe_3, PPh_3, PCy_3.

2. Computational Procedure

All calculations were performed by utilizing the two-layer ONIOM approach.[26,27] In the ONIOM partitioning the studied $[MR_2(PR'_3)_2]$ complexes (L = PR'_3) were divided into two layers: the first layer includes the ligands R, metal center and phosphorus atoms, and the second layer includes the substituents at the phosphane ligands (R′). A graphical representation of the partitioning scheme is given in Scheme 2.

The first layer was treated at the high B3LYP/BSI level. The basis set BSI consists of the SDD basis set[28] for the metal atom and the 6-311G(d) basis set[29] for the other atoms. The second layer was treated at the relatively low HF/Lanl2mb level. Therefore, this two-layer ONIOM approach used in the present study was denoted as ONIOM-(B3LYP/BSI:HF/Lanl2mb) and it was utilized for geometry optimization and frequency calculations throughout the paper, unless otherwise mentioned. Single-point energy calculations were carried out at the ONIOM(B3LYP/BSI:B3-LYP/Lanl2dz) level by using ONIOM(B3LYP/BSI:HF/Lanl2mb)-optimized geometry: this approach was denoted as ONIOM(B3LYP/BSI:B3LYP/Lanl2dz)//ONIOM(B3LYP/BSI:HF/Lanl2mb).

In the ONIOM studies the normal-coordinate analysis has been performed for all stationary points to characterize the nature of TSs and equilibrium structures and to calculate Gibbs free energies (298.15 K, 1 atm, rigid rotor harmonic oscillator approximation). All calculations were performed without symmetry constraints with the Gaussian 03 program.[30] The reliability of the chosen theory level in geometry optimization and energy calculations has been confirmed by a special study (see Supporting Information).

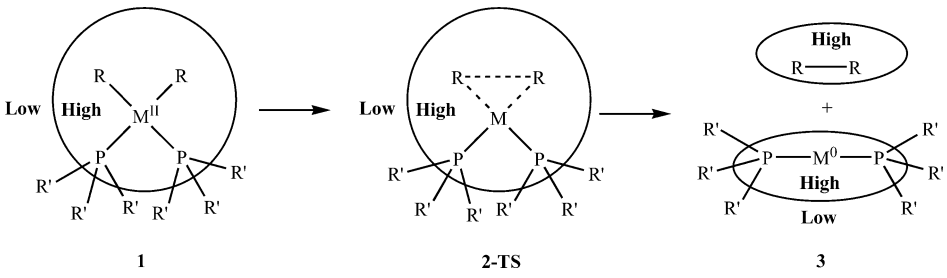

Scheme 2. Model (the first layer, in circle) and real systems used in the ONIOM calculations, which are treated at high and low levels, respectively.

Table 1. Calculated relative energies of the stationary points **1**–**5-TS** on the ΔE, ΔH and ΔG energy surfaces[a,b] [kcal/mol] at 298.15 K and 1 atm; system **A** at the B3LYP/BSI level, systems **B**–**J** at the ONIOM(B3LYP/BSI:B3LYP/Lanl2dz)//ONIOM(B3LYP/BSI:HF/Lanl2mb) level.

System	M	L	R^1	R^2	**1**	**2-TS**	**3**	**4**	**5-TS**
A	Pd	PH_3	Me	Me	0.0/0.0/0.0	25.2/24.2/23.6	–31.4/–30.4/–41.7	17.2/15.0/2.4	29.3/26.9/15.7
B	Pd	PMe_3	Me	Me	0.0/0.0/0.0	30.0/29.1/26.4	–32.4/–31.5/–46.3	20.7/18.8/3.5	33.0/30.8/16.5
C	Pd	PPh_3	Me	Me	0.0/0.0/0.0	23.1/22.2/17.9	–39.2/–38.5/–54.7	13.9/12.1/–6.3	26.2/24.2/6.6
D	Pd	PCy_3	Me	Me	0.0/0.0/0.0	28.8/27.4/25.1	–39.2/–39.6/–56.5	13.3/10.6/–7.2	24.9/21.9/4.8
E	Pd	PPh_3	$CH=CH_2$	$CH=CH_2$	0.0/0.0/0.0	3.7/3.0/2.8	–44.2/–43.7/–59.4	12.0/10.5/–6.6	15.0/13.0/–3.0
F	Pd	PPh_3	Ph	Ph	0.0/0.0/0.0	9.7/8.8/9.3	–43.2/–43.3/–59.6	10.8/9.4/–10.3	14.8/12.7/–4.6
G	Pd	PPh_3	C≡CH	C≡CH	0.0/0.0/0.0	13.3/12.0/10.2	–24.1/–24.4/–40.0	22.2/20.7/3.7	29.4/27.1/10.0
H	Pd	PPh_3	$CH=CH_2$	Me	0.0/0.0/0.0	11.8/11.1/10.4	–40.2/–39.8/–56.3	12.4/10.5/–6.8	19.2/17.1/0.9
I	Pd	PPh_3	$CH=CH_2$	Ph	0.0/0.0/0.0	7.5/6.7/6.7	–42.5/–42.3/–59.4	11.9/10.5/–7.1	15.4/13.4/–2.4
J	Pd	PPh_3	$CH=CH_2$	C≡CH	0.0/0.0/0.0	8.4/7.4/6.7	–31.5/–31.8/–48.4	14.5/12.8/–4.0	21.4/19.0/2.8

[a] The values are provided in the order *E*/*H*/*G*. [b] In the five-coordinate species **4** and **5-TS** the ligand in *trans* position to R^1 was dissociated.

Table 2. Calculated selected bond lengths [Å] and angles [°] for the studied complexes; system **A** at the B3LYP/BSI level, systems **B**–**G** at the ONIOM(B3LYP/BSI:HF/Lanl2mb) level.[a,b]

System	M	L	R^1, R^2	Structure	M–C1[c]	M–C2[c]	M–P1[d]	M–P2[d]	C1–C2[c]	C1–M–C2[c]	P1–M–P2[d]	Tilt angle[e]
A	Pd	PH_3	Me	**1**	2.100	2.100	2.367	2.367	2.778	82.8	102.2	0.8
				2-TS	2.198	2.198	2.384	2.384	2.071	56.2	111.4	52.0
				4	2.047	2.038	2.410	–	2.791	86.2	–	–
				5-TS	2.117	2.167	2.304	–	2.084	58.2	–	–
B	Pd	PMe_3	Me	**1**	2.132	2.132	2.322	2.322	2.774	81.2	107.2	0.1
				2-TS	2.196	2.196	2.331	2.331	2.117	57.6	118.7	59.8
				4	2.053	2.046	2.373	86.2	2.802	86.2	–	–
				5-TS	2.117	2.161	2.290	58.4	2.290	58.4	–	–
C	Pd	PPh_3	Me	**1**	2.123	2.113	2.370	2.376	2.770	81.6	103.2	1.9
				2-TS	2.190	2.190	2.367	2.367	2.113	57.7	122.1	60.7
				4	2.057	2.046	2.383	–	2.788	85.6	–	–
				5-TS	2.125	2.164	2.306	–	2.072	57.8	–	–
D	Pd	PCy_3	Me	**1**	2.127	2.127	2.432	2.432	2.642	76.8	110.1	9.2
				2-TS	2.193	2.197	2.385	2.411	2.109	57.4	120.3	67.6
				4	2.060	2.044	2.392	–	2.771	84.9	–	–
				5-TS	2.124	2.159	2.318	–	2.061	57.5	–	–
E	Pd	PPh_3	$CH=CH_2$	**1**	2.074	2.061	2.374	2.392	2.614	78.4	104.4	3.2
				2-TS	2.091	2.086	2.369	2.383	2.559	57.7	108.7	5.8
				4	2.016	1.991	2.389	–	2.760	87.1	–	–
				5-TS	2.031	2.031	2.362	–	2.151	64.0	–	–
F	Pd	PPh_3	Ph	**1**	2.095	2.076	2.384	2.405	2.694	80.5	104.6	8.5
				2-TS	2.129	2.137	2.401	2.385	1.981	55.3	108.7	16.6
				4	2.029	2.011	2.386	–	2.751	85.8	–	–
				5-TS	2.049	2.066	2.352	–	2.126	62.2	–	–
G	Pd	PPh_3	C≡CH	**1**	2.010	1.999	2.356	2.372	2.724	85.6	104.4	0.3
				2-TS	2.014	2.018	2.388	2.375	1.809	53.3	109.0	1.4
				4	1.981	1.920	2.333	–	2.815	92.3	–	–
				5-TS	1.961	1.948	2.373	–	1.957	60.1	–	–

[a] Length of the formed carbon–carbon bond in organic products R–R: 1.529 (**3_A** to **3_D**), 1.456 (**3_E**), 1.485 (**3_F**), 1.365 (**3_G**); length of the Pd–P bond in the PdL_2 product complexes: 2.289 (**3_A**), 2.286 (**3_B**), 2.295 (**3_C**, **3_E** to **3_G**), 2.315 (**3_D**). [b] The imaginary frequencies [i cm^{-1}] for the transition states **2-TS_A** to **2-TS_G**, respectively: 481, 450, 432, 434, 373, 328, 435; for the transition states **5-TS_A** to **5-TS_G**, respectively: 425, 426, 441, 451, 278, 251, 370. [c] C1 and C2 belong to R^1 and R^2, respectively. [d] P1 is *trans* to C1 and P2 is *trans* to C2. [e] Absolute value of the angle between the P1–M–P2 and C1–M–C2 planes.

The calculated relative energies (ΔE, ΔH, ΔG) of reactants, intermediates, transition states and products are summarized in Table 1, while their most important structural parameters are listed in Table 2. The optimized structures of Me–Me reductive elimination reactions are shown in Figures 1 and 2, and those of the coupling of unsaturated organic groups are given in Figure S1 (see Supporting Information).

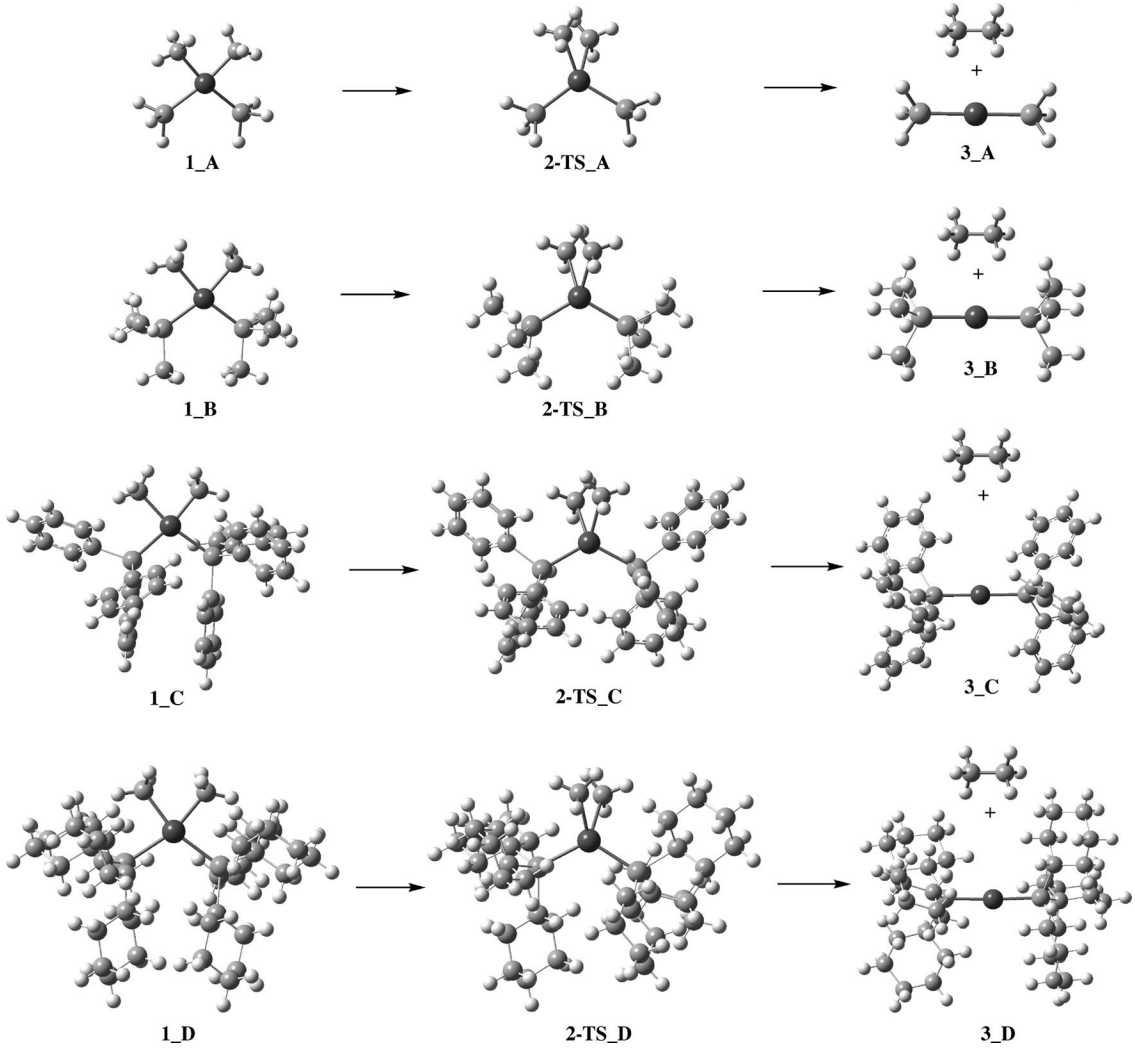

Figure 1. Optimized structures of the initial complexes, transition states and products of the Me–Me coupling from $[Pd(CH_3)_2L_2]$ with different ligands. Their important geometry parameters are given in Table 2 and the energetic data is listed in Table 1.

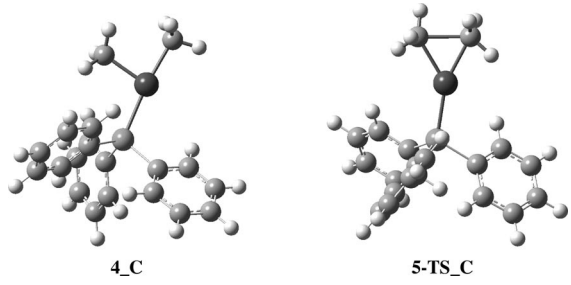

Figure 2. Optimized structures **4_C** and **5-TS_C**. Their important geometry parameters are given in Table 2 and the energetic data is listed in Table 1.

3. Results

First, we analyze the effect of the phosphane ligand on the geometry of the $[Pd(CH_3)_2L_2]$ complexes, followed by a discussion of the potential-energy surfaces of Me–Me coupling for both (four- and three-coordinate) pathways of the reductive elimination reaction. Finally, C–C bond formation between the unsaturated organic groups (vinyl, phenyl and ethynyl) and unsymmetrical couplings will be considered with the triphenylphosphane ligand.

A. Effect of Phosphane Ligands on the Geometry of the $[Pd(CH_3)_2L_2]$ Complexes (1_A to 1_D)

In this section we analyze how sensitive the geometry parameters of the initial metal complexes are to the nature of the phosphane ligands. Both Pd–C and Pd–P bonds will be involved in the comparison. The shortest Pd–C distance was calculated for the L = PH_3 case, and substituted phosphane ligands increased the Pd–C distance by 0.018–0.032 Å (Table 2). The following trend in Pd–C bond length was obtained for the ligands studied (in Å):[31] **1_B** (2.132; L = PMe_3) > **1_D** (2.127; L = PCy_3) > **1_C** (2.118; L = PPh_3) > **1_A** (2.100; L = PH_3).

Alkyl-substituted phosphanes gave longer Pd–C bonds relative to L = PPh_3 and PH_3. The longest Pd–C bond was calculated for L = PMe_3 having the smaller substituent size

as compared to L = PCy_3. However, rather small changes in the bond length do not provide the necessary basis for further analysis. The calculations agree with available experimental data; according to the X-ray studies, M–C_{methyl} distances span a range of 2.08–2.16 Å and are not much sensitive to the identity of the phosphane ligand.[32] Indeed, the influence of the crystal-packing effect may diminish the small differences in M–C bond lengths caused by the ligand effect.

The following trend in Pd–P bond length was calculated for the studied ligands (in Å):[31] **1_D** (2.432; L = PCy_3) > **1_C** (2.373; L = PPh_3) > **1_A** (2.367; L = PH_3) > **1_B** (2.322; L = PMe_3)

Longer Pd–P bonds for L = PCy_3 can be explained by the bulkiness of this ligand. The presence of large steric repulsions in the case of PCy_3 is also evident from increased P–Pd–P angles and decreased C–Pd–C angles, as compared to the other ligands (Table 2). Despite the obvious geometry changes caused by the PCy_3 ligand, the overall trend cannot be easily rationalized. Similar conclusions can be drawn upon analysis of experimental geometries determined in X-ray studies.[32]

B. Effect of the Organic Group on the Geometry of the $[PdR_2(PPh_3)_2]$ Complexes (1_E to 1_J)

The structures **1_E** to **1_G** with unsaturated organic ligands and L = PPh_3 (Table 2) can be compared with similar compounds for L = PH_3 studied earlier.[23] Introducing Ph substituents into the phosphane ligand increased on average the length of the Pd–C bonds by 0.01–0.03 Å, while the trends in the Pd–P distances and P–Pd–P angles were less pronounced; the average changes were <0.02 Å and <1°, respectively.

It is important to point out that the conformational flexibility of PPh_3 caused some deviations towards an asymmetric ligand environment. In fact, Pd–C1 and Pd–C2 bonds, as well as Pd–P1 and Pd–P2 bonds, within the same complex (**1_E** to **1_G**, as well as **1_C**) differ by 0.01–0.02 Å (Table 2). The expected relationship of the shorter Pd–C bond *trans* to the longer Pd–P bond in these complexes originates from the *trans* effect (Table 2). It should be pointed out that experimental X-ray studies have also reported unsymmetrical ligand environments with similar differences in the bond lengths.[32] Finally, in agreement with the discussion in section A, no clear trends between the geometry parameters of the initial complexes and the nature of phosphane ligands can be outlined.

C. Effect of Phosphane Ligands on the Energetics of Reductive Elimination from the Four-Coordinate $[Pd(CH_3)_2L_2]$ Complexes (1_A to 1_D)

The investigated reductive elimination reactions occur by a concerted mechanism (Figure 1). In such a case, movement along the reaction coordinate involves elongation of Pd–C bonds and an increase in P–Pd–P angles, as well as shortening of C–C bonds and a decrease in C–Pd–C angles. Optimized geometry parameters for the initial complexes and transition states reflect these structural changes (Table 2).

According to the calculated barriers ($\Delta H^{\neq}$), the reactivity of the studied complexes in the reductive elimination reaction decreases in the order (Table 1): **1_C** (L = PPh_3) > **1_A** (L = PH_3) > **1_D** (L = PCy_3) > **1_B** (L = PMe_3).

Therefore, the lowest reactivity in C–C bond formation was predicted for the complex with the PMe_3 ligand, while the complex with the PPh_3 ligand should be the most reactive. All reactions are exothermic; energy gain upon product formation follows the trend: **1_C**, **1_D** > **1_A**, **1_B** (Table 1).[33] The calculated ΔE and ΔH values are nearly identical, with a difference of <1.5 kcal/mol. In terms of ΔG the reactions are highly exoergic (due to the entropy contribution as well), and the activation barriers are slightly decreased (Table 1).[34]

The calculated reactivity order can not be easily understood on the basis of the known properties of the ligands. In order to estimate the electronic and steric effects of the ligand on reaction energetics, we have applied decomposition analysis based on ONIOM calculations at different levels (Scheme 3). The system with the simplest ligand (L = PH_3) computed at the MO level was used as a reference point. From the reference point we cannot directly estimate the desired steric and electronic effects in the real chemical system (L = PR'_3) calculated at the ONIOM(MO:MO) level. However, the analysis can be simplified by carrying out ONIOM(MO:MM) calculations on the real systems, for the decomposition point, which includes only the steric effect of substituents R′. The difference between the reference and decomposition points provides information about the steric effect in the studied system, while the electronic effect can be revealed by comparing the real system and the decomposition point (Scheme 3).

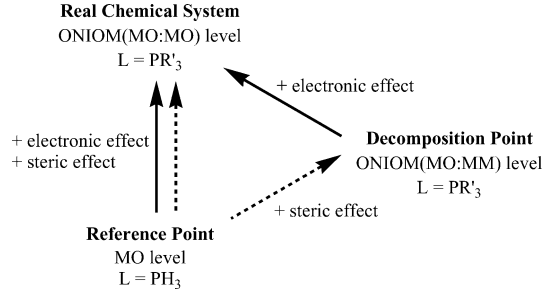

Scheme 3. ONIOM decomposition analysis to evaluate steric and electronic effects of phosphane ligands in the studied complexes.

For the decomposition point, we have carried out single-point ONIOM(B3LYP/BSI:UFF) calculations with the UFF molecular mechanics force field as the low level (Table 3). Comparison of ONIOM(B3LYP/BSI:UFF) energies for L = PMe_3, PPh_3, PCy_3 with the B3LYP/BSI energy for L = PH_3, reveals a small and noncharacteristic change for the PMe_3 ligand, while the activation barriers for the PPh_3 and PCy_3 ligands are decreased by 4–7 kcal/mol (see Tables 1 and 3). This trend is in good qualitative agreement

with the steric bulkiness of the ligands: PCy_3, $PPh_3 > PMe_3 \approx PH_3$.[35]

Table 3. Calculated ΔE relative energies of the stationary points **1**, **2-TS** and **3** at the ONIOM(B3LYP/BSI:UFF)//ONIOM(B3LYP/BSI:HF/Lanl2mb) level [kcal/mol].

System	M	L	R^1, R^2	**1**	**2-TS**	**3**
B	Pd	PMe_3	Me	0.0	26.8	–32.9
C	Pd	PPh_3	Me	0.0	17.8	–46.7
D	Pd	PCy_3	Me	0.0	20.7	–43.8

In the present metal complexes, the steric effect includes repulsion between the phosphane ligands and between the phosphane and CH_3 ligands. These steric repulsions destabilize both the initial complex **1** and the transition state **2-TS**. The decrease in the activation barrier ($\Delta E^{\neq}$) at the ONIOM(B3LYP/BSI:UFF) level suggests that the initial complex **1** is more destabilized by the steric repulsions relative to the transition state **2-TS**.[36] This energy trend is in excellent agreement with geometry parameters, because in the transition state both P–Pd–P and P–Pd–C_{cis} angles become larger. The energy gain (ΔE) calculated at the ONIOM(B3LYP/BSI:UFF) level is almost the same for the PMe_3 ligand and significantly higher for the PPh_3 and PCy_3 ligands relative to the ONIOM(B3LYP/BSI:B3LYP/Lanl2dz) level (see Tables 1 and 3, respectively), which is also evident from minimizing steric repulsions in **3**.

Now we can consider the influence of the electronic effect. In the present system the interaction between the phosphane ligand and the metal center affects both the initial complex and the transition state. The nature of the electronic effect can be revealed by comparative analysis of the ONIOM(B3LYP/BSI:UFF) energy surface, which includes only the steric effect, and the ONIOM(B3LYP/BSI:B3LYP/Lanl2dz) energy surface, which includes both electronic and steric effects. Comparison of the ONIOM(B3LYP/BSI:-UFF) and ONIOM(B3LYP/BSI:B3LYP/Lanl2dz) energies [both evaluated by using the same ONIOM(B3LYP/BSI:HF/Lanl2mb) optimized geometries] has shown that for L = PMe_3, PPh_3, PCy_3, inclusion of the electronic effects increased the activation barriers by 3–8 kcal/mol (see Tables 1 and 3, respectively). This suggests that electronic effects may have more influence on the transition state than on the initial complex.[37] It appears that the weak metal–carbon bond in the transition state is more sensitive to the electronic effect than the relatively strong bond of the initial complex.

D. Reductive Elimination from the Three-Coordinate $[Pd(CH_3)_2L]$ Complexes (4_A to 4_D) by the Phosphane Ligand Predissociation Mechanism

Another pathway of C–C bond formation may involve phosphane ligand dissociation **1** → **4** followed by **4** → **5-TS** reductive elimination (Scheme 1). Reassociation of the phosphane ligand after releasing the organic product results in the same product, **3**.[38] An example of the optimized structures of **4_C** and **5-TS_C** is shown in Figure 2. Complex **4_C** affords T-shaped geometry with nonequivalent Pd–C bonds, which is shifted towards Y-shaped geometry upon moving to **5-TS_C**. However, the transition-state structure did not become symmetric as was evident from different Pd–C1 and Pd–C2 bond lengths (Table 2) and P–Pd–C angles.[39] Similar geometry changes were also observed for the other three-coordinate structures considered in the present study. Comparing corresponding **2-TS** and **5-TS** geometries, one may clearly notice an earlier character for **5-TS** (shorter Pd–C bonds and longer C–C bonds for **5-TS**, see Table 2).

In agreement with geometry trends, phosphane ligand predissociation significantly lowers activation energies of the reductive elimination process. The calculated **4** → **5-TS** activation barriers on the ΔE, ΔH and ΔG surfaces have similar values in the range 11–13 kcal/mol for all of the studied complexes (**4_A** to **4_D**), which are much smaller than **1** → **2-TS** activation barriers of $\Delta H^{\neq}$ = 22–29 kcal/mol (**1_A** to **1_D**). Therefore, if monoligated $[PdR_2L]$ species **4** would be involved as the initial complexes (in such a case ligand predissociation is not required) in the C–C reductive elimination, the reaction would be faster and less sensitive to the ligand effects. In the case of four-coordinate initial complexes the activation barriers **1** → **5-TS** should be considered to estimate the relative reactivity order (because **4** is higher in energy than **1** on the ΔH surface), which follows the trend (see Table 1): L = PCy_3 > PPh_3 > PH_3 > PMe_3.

As evident from Table 1, the potential surface is dramatically influenced by the value of the Pd–P bond energy (energy difference between **4** and **1**). The calculated Pd–P bond energy (in ΔH) for the first phosphane ligand dissociation from the $[Pd(CH_3)_2L_2]$ complexes **1_A** to **1_D** decreases in the order: PMe_3 (18.8 kcal/mol) > PH_3 (15.0 kcal/mol) > PPh_3 (12.1 kcal/mol) > PCy_3 (10.6 kcal/mol).

Comparison of the PH_3 and PMe_3 ligands (both having relatively small steric effects) indicates that electron donation from the ligand to the metal center increases the Pd–P bond energy in the present complexes. However, for the more bulky PCy_3 ligand, the steric repulsions in **1** decrease the Pd–P bond energy and facilitate phosphane ligand dissociation. As a result, carbon–carbon bond formation through the **1** → **4** → **5-TS** → **3** pathway for L = PCy_3 is energetically even less demanding than that through the **1** → **2-TS** → **3** pathway for L = PPh_3 ($\Delta H^{\neq}$ = 21.9 and 22.2 kcal/mol, respectively). The entropy contribution should provide additional energetic favor to the dissociation pathway on the ΔG surface.[34]

E. Reductive Elimination of Unsaturated Vinyl, Phenyl and Ethynyl Groups from the Four-Coordinate $[PdR_2(PPh_3)_2]$ Complexes (1_E to 1_G) and the Three-Coordinate $[PdR_2PPh_3]$ Complexes (4_E to 4_G)

Vinyl–vinyl, phenyl–phenyl and ethynyl–ethynyl couplings on Pd^{II} centers with the PPh_3 ligand also proceeded through the concerted transition states (Figure S1, Supporting Information). However, these reductive elimination re-

actions require the overcoming of smaller activation barriers (Table 1). According to the calculated $\Delta H^{\neq}$ values, the reactivity in C–C bond formation among the present complexes follows the trend: **1_E** (vinyl–vinyl) > **1_F** (Ph–Ph) > **1_G** (ethynyl–ethynyl) > **1_C** (Me–Me). The formation of buta-1,3-diene (**3_E**) and biphenyl (**3_F**) is exothermic by $\Delta H \approx$ –43 kcal/mol; the formation of buta-1,3-diyne (**1_G**) is less exothermic with ΔH = –24.4 kcal/mol.[40]

The Pd–P bond energy increases in the order (ΔH [kcal/mol]): **1_F** (9.4) < **1_E** (10.5) << **1_G** (20.7) for the vinyl, phenyl and ethynyl complexes, respectively (Table 1). The higher bond energy in the case **1_G** is consistent with the shorter Pd–P bond in this compound (Table 2). Therefore, according to the calculated energetics (Table 1), vinyl–vinyl and Ph–Ph couplings are likely to involve the three-coordinate reaction pathway (**1** → **4** → **5-TS** → **3**), while ethynyl–ethynyl coupling should follow the standard pathway with four-coordinate species (**1_G** → **2-TS_G** → **3_G**). The calculated energetic trend is in excellent agreement with available experimental studies showing that $[Pd(CH_3)_2L_2]$ complexes are rather stable in solution, whereas analogous diphenylpalladium complexes are unstable.[17d,41] It has also been shown that replacement of Me groups by Ph groups in the PMe_xPh_{3-x} ligands increases the rate of C–C bond formation within the catalytic cross-coupling cycle.[1d]

F. Unsymmetrical Coupling of Methyl–Vinyl, Phenyl–Vinyl and Ethynyl–Vinyl Groups from the Four-Coordinate $[PdR^1R^2(PPh_3)_2]$ Complexes (1_H to 1_J) and the Three-Coordinate $[PdR^1R^2PPh_3]$ Complexes (4_H to 4_J)

Reductive elimination of Me and vinyl groups by the four-coordinate pathway (**1_H** → **2-TS_H** → **3_H**) requires overcoming the activation barrier of $\Delta H^{\neq}$ = 11.1 kcal/mol and is exothermic by ΔH = –39.8 kcal/mol (Table 1). These values are intermediate between the vinyl–vinyl ($\Delta H^{\neq}$ = 3.0 kcal/mol, ΔH = –43.7 kcal/mol) and Me–Me ($\Delta H^{\neq}$ = 22.2 kcal/mol, ΔH = –38.5 kcal/mol) couplings. Thus, the following relative reactivity should be expected: vinyl–vinyl > vinyl–Me > Me–Me. The same relationship was calculated for the other studied unsymmetrical couplings: the vinyl–Ph coupling is intermediate between the vinyl–vinyl and Ph–Ph couplings, and the vinyl–ethynyl coupling is intermediate between the vinyl–vinyl and ethynyl–ethynyl couplings (Table 1).

Remarkably, this tendency remains valid for the three-coordinate pathway,[42] although the difference in activation barriers was rather small (**4** → **5-TS**; ΔH [kcal/mol]): vinyl–vinyl (2.5) > vinyl–Me (6.6) > Me–Me (12.1); vinyl–vinyl (2.5) > vinyl–Ph (2.9) > Ph–Ph (3.3); vinyl–vinyl (2.5) > vinyl–ethynyl (6.2) > ethynyl–ethynyl (6.4).

Geometry parameters are in line with the energy data and follow the trends discussed above; optimized geometry parameters are listed in Table S1 (see Supporting Information).

4. Discussion

It was shown that geometry parameters of initial $[PdR_2L_2]$ complexes are not very sensitive to the nature of the phosphane ligands. Therefore, electronic and steric properties derived from the initial metal complexes or from the free ligands should be used with care for predicting the reactivity of transition-metal complexes. Moreover, the calculations have shown that the influence of the conformational changes on geometry may be of the same order of magnitude as the ligand effects.

Applying ONIOM decomposition analysis, we have found that the steric effect of phosphane ligands mostly influences the initial Pd^{II} complex, while the electronic effect has the greatest impact on the transition state. The larger steric effect of R′ decreases the activation barriers of C–C reductive elimination. The electronic effect changes the reactivity in the opposite manner: inclusion of the electronic effect increases the activation barriers.

In sections 2C and 2D we have analyzed the four-coordinate and three-coordinate pathways separately; here we provide a joint analysis of both pathways to predict the overall reactivity in the studied system. The reductive elimination reaction from Pd^{II} complexes by the four-coordinative pathway follows the trend: L = PPh_3 > PH_3 > PCy_3 > PMe_3. However, in the case of the three-coordinate pathway the complex with the tricyclohexylphosphane ligand becomes more reactive: L = PCy_3 > PPh_3 > PH_3 > PMe_3.[43] The relative reactivity through these two pathways is determined by the strength of the metal–phosphorus bond. The calculated Pd–P bond dissociation enthalpy for $[Pd(CH_3)_2L_2]$ decreases in the order: L = PMe_3 > PH_3 > PPh_3 > PCy_3. Easy dissociation of the PCy_3 ligand favors C–C coupling by the three-coordinate pathway. Considering both potential energy surfaces, for L = PCy_3 the reaction is most likely to undergo the three-coordinate predissociation pathway involving T-shaped complexes, for L = PH_3 and L = PMe_3 the classical four-coordinate pathway, and for L = PPh_3 both pathways should be accessible.

The results of theoretical studies of C–H reductive elimination from platinum complexes with PH_3 and PMe_3 ligands[19] are in excellent agreement with our study of C–C bond formation on Pd; for these ligands the four-coordinate pathway should be preferred. At the same time, this indicates that for studies of the ligand effect, PH_3 and PMe_3 are unreliable models of PPh_3 and PCy_3. Explicit consideration of substituents is required to obtain agreement with experiment.

Coupling of different organic groups from $[PdR_2(PPh_3)_2]$ complexes was predicted to be in the following reactivity order: vinyl–vinyl > Ph–Ph > ethynyl–ethynyl > Me–Me for the four-coordinate pathway and vinyl–vinyl, Ph–Ph > Me–Me > ethynyl–ethynyl for the three-coordinate pathway. The Pd–P bond dissociation enthalpy depends on the nature of the organic group being eliminated that is attached to the palladium atom as was calculated for the series of $[PdR_2(PPh_3)_2]$ complexes: R = Me, ethynyl > Ph, vinyl. Therefore, vinyl–vinyl and Ph–Ph couplings are

likely to proceed by the three-coordinate predissociation pathway; however, ethynyl–ethynyl coupling can start directly from the four-coordinate complex.

Special note should be made concerning the solvent effect. Using PCM calculations it was reported that the solvent effect does not change in a substantial manner the potential energy surfaces of four-coordinate reductive elimination pathways involving neutral metal complexes.[22] In case of the predissociation pathway, the solvent could coordinate to a vacancy in the metal center. However, taking into account that most organic solvents (toluene, benzene, dichloromethane, chloroform, hexanes, etc.) are weakly coordinated to a metal center, this process is unlikely to introduce principal changes to the mechanism.[44]

5. Conclusions

The study has clearly shown that the ligand effect on C–C bond formation should be considered in view of the reaction mechanism, otherwise it may be a source of inconsistencies or even erroneous conclusions. The influence of steric and electronic factors depends on the nature of reacting species and the ligand environment as well as the type of organic groups being eliminated.

The calculations revealed that different ligands may involve different mechanisms of the C–C reductive elimination reaction. Among the ligands studied, PCy_3 should be used to facilitate the T-shaped pathway by the predissociation mechanism and increase the reactivity. The PMe_3 ligand should be utilized for stabilizing the four-coordinate complexes and decrease the reactivity in reductive elimination reactions. The PPh_3 ligand represents a more universal choice, since it showed good reactivity for both mechanisms.

According to the calculated activation barriers, the relative reactivity orders were found for a series of C–C coupling reactions involving various organic groups. Particularly, for the four-coordinate pathway: vinyl–vinyl > vinyl–Ph > vinyl–ethynyl > Ph–Ph > vinyl–Me > ethynyl–ethynyl > Me–Me; and for the three-coordinate pathway: vinyl–vinyl > vinyl–Ph > vinyl–ethynyl, Ph–Ph > vinyl–Me, ethynyl–ethynyl > Me–Me. The relative reactivity orders for both pathways coincide, except that rather small activation barriers in the latter case did not allow us to draw a clear distinction for some reactions.

Finally, we would like to point out that ONIOM calculations provide reliable results not only for the evaluation of geometries and energy data, but also for analyzing electronic and steric effects. ONIOM partitioning to high and low levels gives a flexible tool to define a region of interest, whose steric and electronic properties are analyzed.

Supporting Information (see footnote on the first page of this article): Testing the reliability of geometry optimization (Section 1). Testing the reliability of energy calculations (Section 2). Optimized structures of the initial complexes, transition states and products for vinyl–vinyl, Ph–Ph and ethynyl–ethynyl coupling from $[PdR_2(PPh_3)_2]$ (Figure S1); their important geometry parameters are given in Table 2 and the energetic data is listed in Table 1. The calculated selected bond lengths [Å] and angles [°] for the systems **H**–**J** at the ONIOM(B3LYP/BSI:HF/Lanl2MB) level (Table S1).

Acknowledgments

V. P. A. acknowledges the Visiting Fellowship at the Cherry L. Emerson Center of Emory University.

[1] a) J. Tsuji, *Transition Metal Reagents and Catalysts: Innovations in Organic Synthesis*, John Wiley & Sons, Chichester, **2000**; b) *Handbook of organopalladium chemistry for organic synthesis* (Ed.: E. Negishi), John Wiley & Sons, New York, Chichester, **2002**, vol. 1, pp. 215–994; c) M. Beller, C. Bolm, *Transition Metals for Organic Chemistry*, Wiley-VCH: Weinheim, **1998**; d) *Metal-catalyzed Cross-coupling Reactions* (Eds.: F. Diederich, P. J. Stang), Wiley-VCH, Weinheim, **1998**.

[2] a) I. P. Beletskaya, A. V. Cheprakov, "Metal complexes as catalysts for C-C cross-coupling reactions", in *Comprehensive Coordination Chemistry II* (Eds.: J. A. McCleverty, T. J. Meyer), Elsevier Ltd., Oxford, **2004**, vol. 9, pp. 305–368; b) N. Miyaura, A. Suzuki, *Chem. Rev.* **1995**, *95*, 2457; c) N. Miyaura, *J. Organomet. Chem.* **2002**, *653*, 54; d) V. Farina, V. Krishnamurthy, W. J. Scott, "The Stille Reaction", in *Organic Reactions*, John Wiley & Sons Inc., New York, **1997**, vol. 50; e) K. Kugami, M. Kosugi, *Top. Curr. Chem.* **2002**, *219*, 87.

[3] a) A. Togni, H. Grützmacher (Eds.), *Catalytic Heterofunctionalization*, Wiley-VCH, Weinheim, **2001**; b) M. Beller, J. Seayad, A. Tillack, H. Jiao, *Angew. Chem. Int. Ed.* **2004**, *43*, 3368; c) I. Beletskaya, C. Moberg, *Chem. Rev.* **2006**, *106*, 2320; d) F. Alonso, I. P. Beletskaya, M. Yus, *Chem. Rev.* **2004**, *104*, 3079.

[4] a) J. Louie, J. F. Hartwig, *Tetrahedron Lett.* **1995**, *36*, 3609; b) A. S. Guram, R. A. Rennels, S. L. Buchwald, *Angew. Chem. Int. Ed. Engl.* **1995**, *34*, 1348; c) J. F. Hartwig, *Inorg. Chem.* **2007**, *46*, 1936; d) J. P. Wolfe, S. Wagaw, J.-F. Marcoux, S. L. Buchwald, *Acc. Chem. Res.* **1998**, *31*, 805.

[5] From the chemical and industrial points of view readily available and cheap organic chlorides are the best starting materials for catalytic C–C and C–X bond formation. Not surprisingly, activation of organic chlorides is one of the most actively studied areas of transition-metal catalysis.

[6] For a recent review, see: S. P. Nolan, O. Navarro, "C–C Bond Formation by Cross-Coupling" in *Comprehensive Organometallic Chemistry III* (Eds.: D. M. P. Mingos, R. H. Crabtree), Elsevier Ltd., Oxford, **2007**, vol. 11, pp. 1–37.

[7] Selected representative examples: a) S. D. Walker, T. E. Barder, J. R. Martinelli, S. L. Buchwald, *Angew. Chem. Int. Ed.* **2004**, *43*, 1871; b) A. F. Littke, C. Dai, G. Fu, *J. Am. Chem. Soc.* **2000**, *122*, 4020; c) J. P. Stambuli, R. Kuwano, J. F. Hartwig, *Angew. Chem. Int. Ed.* **2002**, *41*, 4746; d) A. Zapf, A. Ehrentraut, M. Beller, *Angew. Chem. Int. Ed.* **2000**, *39*, 4153; e) V. P. W. Bohm, C. W. K. Gstottmayr, T. Weskamp, W. A. Herrmann, *J. Organomet. Chem.* **2000**, *595*, 186; f) A. Zapf, M. Beller, *Chem. Eur. J.* **2000**, *6*, 1830; g) J. P. Wolfe, R. A. Singer, B. H. Yang, S. L. Buchwald, *J. Am. Chem. Soc.* **1999**, *121*, 9550; h) X. Bei, H. W. Turner, W. H. Weinberg, A. S. Guram, *J. Org. Chem.* **1999**, *64*, 6797; i) C. Zhang, J. Huang, M. L. Trudell, S. P. Nolan, *J. Org. Chem.* **1999**, *64*, 3804; j) A. F. Littke, G. Fu, *Angew. Chem. Int. Ed.* **1998**, *37*, 3387.

[8] Theoretical studies of the mechanism of cross-coupling reactions with PH_3 and PMe_3 model ligands: a) R. Alvarez, O. N. Faza, A. R. de Lera, D. J. Cardenas, *Adv. Synth. Catal.* **2007**, *349*, 887; b) A. A. C. Braga, G. Ujaque, F. Maseras, *Organometallics* **2006**, *25*, 3647; c) A. A. C. Braga, N. H. Morgon, G. Ujaque, F. Maseras, *J. Am. Chem. Soc.* **2005**, *127*, 9298; d) R. Alvarez, O. N. Faza, C. S. López, A. R. de Lera, *Org. Lett.* **2006**, *8*, 35; e) A. Ariafard, Z. Lin, I. J. S. Fairlamb, *Organometallics* **2006**, *25*, 5788; f) E. Napolitano, V. Farina, M. Persico, *Organometallics* **2003**, *22*, 4030.

[9] Representative theoretical studies of C–halogen bond activation related to cross-coupling reactions: a) M. Ahlquist, P.-O. Norrby, *Organometallics* **2007**, *26*, 550; b) M. Ahlquist, P. Fristrup, D. Tanner, P.-O. Norrby, *Organometallics* **2006**, *25*, 2066; c) L. J. Goossen, D. Koley, H. L. Hermann, W. Thiel, *Organometallics* **2005**, *24*, 2398; d) T. R. Cundari, J. Deng, *J. Phys. Org. Chem.* **2005**, *18*, 417; e) H. M. Senn, T. Ziegler, *Organometallics* **2004**, *23*, 2980; f) A. Sundermann, J. M. L. Martin, *Chem. Eur. J.* **2001**, *7*, 1703.

[10] Selected references: a) C. A. Tolman, *Chem. Rev.* **1977**, *77*, 313; b) W. Strohmeier, F.-J. Muller, *Chem. Ber.* **1967**, *100*, 2812; c) W. Strohmeier, F.-J. Muller, *Z. Naturforsch., Teil B* **1967**, *22*, 451; d) G. M. Bodner, M. Gaul, *J. Organomet. Chem.* **1975**, *101*, 63; e) G. M. Bodner, *Inorg. Chem.* **1975**, *14*, 2694; f) T. A. Mastryukova, M. I. Kabachnik, *Russ. Chem. Rev.* **1969**, *38*, 795; g) W. A. Henderson, C. A. Streuli, *J. Am. Chem. Soc.* **1960**, *82*, 5791; h) A. L. Fernandez, C. Reyes, A. Prock, W. P. Giering, *Organometallics* **1998**, *17*, 2503; i) A. L. Fernandez, T. Y. Lee, C. Reyes, A. Prock, W. P. Giering, C. M. Haar, S. P. Nolan, *J. Chem. Soc. Perkin Trans. 2* **1999**, 2631; j) D. R. Anton, R. H. Crabtree, *Organometallics* **1983**, *2*, 621; k) L. Perrin, E. Clot, O. Eisenstein, J. Loch, R. H. Crabtree, *Inorg. Chem.* **2001**, *40*, 5806; l) K. D. Cooney, T. R. Cundari, N. W. Hoffman, K. A. Pittard, M. D. Temple, Y. Zhao, *J. Am. Chem. Soc.* **2003**, *125*, 4318; m) S. Otto, A. Roodt, *Inorg. Chim. Acta* **2004**, *357*, 1; n) M. Yamanaka, A. Shiga, *J. Theor. Comput. Chem.* **2005**, *4*, 345.

[11] Reviews: a) K. A. Bunten, L. Z. Chen, A. L. Fernandez, A. J. Poe, *Coord. Chem. Rev.* **2002**, *233*, 41; b) D. White, N. J. Coville, "Quantification of Steric Effects in Organometallic Chemistry" in *Advances in Organometallic Chemistry*, Elsevier, New York, **1994**, vol. 36, pp. 95–158; c) T. L. Brown, K. J. Lee, *Coord. Chem. Rev.* **1993**, *128*, 89.

[12] a) C. M. Haar, S. P. Nolan, W. J. Marshall, K. G. Moloy, A. Prock, W. P. Giering, *Organometallics* **1999**, *18*, 474; b) D. C. Smith Jr, C. M. Haar, E. D. Stevens, S. P. Nolan, J. W. Marshall, K. G. Moloy, *Organometallics* **2000**, *19*, 1427.

[13] C. H. Suresh, N. Koga, *Inorg. Chem.* **2002**, *41*, 1573.

[14] W. P. Giering, A. Prock, A. L. Fernandez, *Inorg. Chem.* **2003**, *42*, 8033.

[15] C. H. Suresh, *Inorg. Chem.* **2006**, *45*, 4982.

[16] O. Kuhl, *Coord. Chem. Rev.* **2005**, *249*, 693.

[17] a) B. S. Williams, K. I. Goldberg, *J. Am. Chem. Soc.* **2001**, *123*, 2576; b) D. M. Crumpton-Bregel, K. I. Goldberg, *J. Am. Chem. Soc.* **2003**, *125*, 9442; c) W. J. Marshall, V. V. Grushin, *Organometallics* **2003**, *22*, 1591; d) A. Gillie, J. K. Stille, *J. Am. Chem. Soc.* **1980**, *102*, 4933; e) P. Dierkes, P. W. N. M. van Leeuwen, *J. Chem. Soc. Dalton Trans.* **1999**, 1519; f) G. Mann, D. Baranano, J. F. Hartwig, A. L. Rheingold, I. A. Guzei, *J. Am. Chem. Soc.* **1998**, *120*, 9205; g) J. E. Marcone, G. K. Moloy, *J. Am. Chem. Soc.* **1998**, *120*, 8527.

[18] P. Espinet, A. M. Echavarren, *Angew. Chem. Int. Ed.* **2004**, *43*, 4704.

[19] a) K. L. Bartlett, K. I. Goldberg, T. Borden, *J. Am. Chem. Soc.* **2000**, *122*, 1456; b) K. L. Bartlett, K. I. Goldberg, T. Borden, *Organometallics* **2001**, *20*, 2669.

[20] For representative studies, see: a) K. Tatsumi, R. Hoffmann, A. Yamamoto, J. K. Stille, *Bull. Chem. Soc. Jpn.* **1981**, *54*, 1857; b) J. L. Low, W. A. Goddard, *J. Am. Chem. Soc.* **1986**, *108*, 6115; c) J. L. Low, W. A. Goddard, *Organometallics* **1986**, *5*, 609; d) N. Koga, K. Morokuma, *Organometallics* **1991**, *10*, 946; e) M. R. A. Blomberg, P. E. M. Siegbahn, U. Nagashima, J. Wennerberg, *J. Am. Chem. Soc.* **1991**, *113*, 424; f) P. E. M. Siegbahn, M. R. A. Blomberg, *J. Am. Chem. Soc.* **1992**, *114*, 10548; g) S. Sakaki, M. Ieki, *J. Am. Chem. Soc.* **1993**, *115*, 2373; h) S. Sakaki, M. Ogawa, Y. Musashi, T. Arai, *Inorg. Chem.* **1994**, *33*, 1660; i) S. Sakaki, N. Mizoe, Y. Musashi, B. Biswas, M. Sugimoto, *J. Phys. Chem. A* **1998**, *102*, 8027; j) G. S. Hill, R. J. Puddephatt, *Organometallics* **1998**, *17*, 1478; k) Z. Cao, M. B. Hall, *Organometallics* **2000**, *19*, 3338; l) S. A. Macgregor, G. W. Neave, C. Smith, *J. Chem. Soc. Faraday Trans.* **2003**, *124*, 111.

[21] For general reviews, see: a) A. Didieu, *Chem. Rev.* **2000**, *100*, 543; b) D. G. Musaev, K. Morokuma, *Top. Catal.* **1999**, *7*, 107; c) P. E. M. Siegbahn, M. R. A. Blomberg, in *Theoretical Aspects of Homogeneous Catalysis, Applications of Ab initio Molecular Orbital Theory* (Eds.: P. W. N. M. van Leeuwen, J. H. van Lenthe, K. Morokuma), Kluwer Academic Publishers, Dordrecht, The Netherlands, **1995**; d) N. Koga, K. Morokuma, *Chem. Rev.* **1991**, *91*, 823.

[22] Vinyl–vinyl coupling: a) V. P. Ananikov, D. G. Musaev, K. Morokuma, *J. Am. Chem. Soc.* **2002**, *124*, 2839; b) V. P. Ananikov, D. G. Musaev, K. Morokuma, *Organometallics* **2001**, *20*, 1652.

[23] Coupling of sp^3, sp^2 and sp carbon atoms: V. P. Ananikov, D. G. Musaev, K. Morokuma, *Organometallics* **2005**, *24*, 715.

[24] Theoretical study of reductive elimination of organic molecules from palladium(II) complexes with chelate ligands: E. Zuiderma, P. W. N. M. van Leeuwen, C. Bo, *Organometallics* **2005**, *24*, 3703.

[25] An example of the ligand effect studied for gold(I) complexes: a) O. D. Häberlen, S. C. Chung, N. Rösch, *Int. J. Quantum Chem.* **1994**, *28*, 595; b) O. D. Häberlen, N. Rösch, *J. Phys. Chem.* **1993**, *97*, 4970.

[26] a) S. Dapprich, I. Komáromi, K. S. Byun, K. Morokuma, M. J. Frisch, *J. Mol. Struct. (Theochem)* **1999**, *462*, 1; b) T. Vreven, K. Morokuma, *J. Comput. Chem.* **2000**, *21*, 1419.

[27] V. P. Ananikov, R. Szilagyi, K. Morokuma, D. G. Musaev, *Organometallics* **2005**, *24*, 1938.

[28] a) P. Schwerdtfeger, M. Dolg, W. H. Schwarz, G. A. Bowmaker, P. D. W. Boyd, *J. Chem. Phys.* **1989**, *91*, 1762; b) D. Andrae, U. Haubermann, M. Dolg, H. Stoll, H. Preuss, *Theor. Chim. Acta* **1990**, *77*, 123; c) A. Bergner, M. Dolg, W. Küchle, H. Stoll, H. Preuss, *Mol. Phys.* **1993**, *80*, 1431.

[29] R. Krishnan, J. S. Binkley, R. Seeger, J. A. Pople, *J. Chem. Phys.* **1980**, *72*, 650.

[30] M. J. Frisch, G. W. Trucks, H. B. Schlegel, G. E. Scuseria, M. A. Robb, J. R. Cheeseman, J. A. Montgomery, Jr., T. Vreven, K. N. Kudin, J. C. Burant, J. M. Millam, S. S. Iyengar, J. Tomasi, V. Barone, B. Mennucci, M. Cossi, G. Scalmani, N. Rega, G. A. Petersson, H. Nakatsuji, M. Hada, M. Ehara, K. Toyota, R. Fukuda, J. Hasegawa, M. Ishida, T. Nakajima, Y. Honda, O. Kitao, H. Nakai, M. Klene, X. Li, J. E. Knox, H. P. Hratchian, J. B. Cross, V. Bakken, C. Adamo, J. Jaramillo, R. Gomperts, R. E. Stratmann, O. Yazyev, A. J. Austin, R. Cammi, C. Pomelli, J. W. Ochterski, P. Y. Ayala, K. Morokuma, G. A. Voth, P. Salvador, J. J. Dannenberg, V. G. Zakrzewski, S. Dapprich, A. D. Daniels, M. C. Strain, O. Farkas, D. K. Malick, A. D. Rabuck, K. Raghavachari, J. B. Foresman, J. V. Ortiz, Q. Cui, A. G. Baboul, S. Clifford, J. Cioslowski, B. B. Stefanov, G. Liu, A. Liashenko, P. Piskorz, I. Komaromi, R. L. Martin, D. J. Fox, T. Keith, M. A. Al-Laham, C. Y. Peng, A. Nanayakkara, M. Challacombe, P. M. W. Gill, B. Johnson, W. Chen, M. W. Wong, C. Gonzalez, J. A. Pople, *Gaussian 03*, rev. C1, Gaussian, Inc., Wallingford, CT, **2004**,.

[31] The averaged value for **1_C** has been used (see Table 2); see discussion below concerning an asymmetric ligand environment.

[32] a) J. C. Thomas, J. C. Peters, *J. Am. Chem. Soc.* **2003**, *125*, 8870; b) S. M. Reid, J. T. Mague, M. J. Fink, *J. Am. Chem. Soc.* **2001**, *123*, 4081; c) J. Ledford, C. S. Shultz, D. P. Gates, P. S. White, J. M. DeSimone, M. Brookhart, *Organometallics* **2001**, *20*, 5266; d) A. S. Abu-Surrah, T. Debaerdemaeker, W. Huhn, B. Rieger, M. Klinga, T. Repo, M. Leskela, *Acta Crystallogr., Sect. C* **2000**, *56*, e42; e) W. De Graaf, J. Boersma, W. J. J. Smeets, A. L. Spek, G. Van Koten, *Organometallics* **1989**, *8*, 2907; f) J. M. Wisner, T. J. Bartczak, J. A. Ibers, J. J. Low, W. A. Goddard III, *J. Am. Chem. Soc.* **1986**, *108*, 347; g) J. M. Wisner, T. J. Bartczak, J. A. Ibers, *Organometallics* **1986**, *5*, 2044; h) see also ref.[12] and discussion therein.

[33] In the present study we do not consider the intermediate σ or π complexes, which may lie on the potential energy surface

between **2-TS** and **3**. Stationary point **3** is of most practical importance, since it corresponds to the product-releasing stage of the catalytic reactions. Numerous studies on the structure and stability of σ or π complexes are already available in the literature (see, for example refs.[20–23]).

[34] It should be noted that gas-phase calculations may overestimate the entropy contribution. For that reason we mainly involve the Δ*H* surface in the discussion. Although, it is clearly established that the dissociation process in solution is more favorable on the Δ*G* surface.

[35] An exact quantitative estimation is unlikely to be obtained in this simple comparison scheme.

[36] An opposite case (if TS is more destabilized than the initial complex) would lead to an increase in the activation energy.

[37] An important issue, which should also be considered for the precise evaluation of the electronic and steric effects by this method, is the quality of the force field (for instance, in terms of the correct reproduction of nonbonded repulsions, etc.). The ONIOM(B3LYP:UFF) level covers a broad range of systems and was utilized in the present study; however, further clarification may be required to investigate the scope of this approach in more detail.

[38] In this case intermediate σ or π complexes may undergo a ligand-substitution reaction (see also ref.[33]).

[39] Values of the P–Pd–C1 and P–Pd–C2 angles [°]: 160.0, 138.0 (**5-TS_A**); 163.1, 138.5 (**5-TS_B**); 160.9, 141.3 (**5-TS_C**); 159.4, 143.1 (**5-TS_D**). Steric bulkiness of the ligands decreases the difference between these angles: 26.0 (**5-TS_A**); 24.6 (**5-TS_B**); 19.6 (**5-TS_C**); 16.3 (**5-TS_D**).

[40] Similar reaction and activation energy changes were predicted for the complexes with PH_3 ligands analyzed in detail earlier (see ref.[23]). Therefore, we do not concentrate on the differences between the organic groups, the phosphane ligand effect will be considered instead.

[41] A. Moravskiy, J. K. Stille, *J. Am. Chem. Soc.* **1981**, *103*, 4182.

[42] In the calculations of the three-coordinate pathway we assume dissociation of the phosphane ligand *trans* to the vinyl group, because the Pd–P bond was calculated to be relatively weaker for that case.

[43] Under experimental conditions these pathways may be switched by addition of an excess of phosphane ligand (to retard ligand dissociation from the Pd complex and favor the four-coordinate pathway) or by using low-ligated palladium species (to facilitate the three-coordinate pathway).

[44] Due to the high *trans* effect of the σ-bonded carbon ligand the solvent molecule most likely will dissociate prior to C–C reductive elimination, which in such a case will undergo the same **4** → **5-TS** → **3** pathway. If the solvent molecule remains coordinated, this will correspond to an intermediate case between the strongly bound phosphane ligand (**1** → **2-TS** → **3** pathway) and the three-coordinate pathway (**4** → **5-TS** → **3**).

Received: August 15, 2007
Published Online: October 12, 2007

